Methodological error and spatial variability of organ blood flow measurements using radiolabeled microspheres*

B. Zwissler[1], R. Schosser[2], C. Weiss[2], V. Iber[2], M. Weiss[2], C. Schwickert[2], P. Spengler[2], and K. Messmer[2]

[1]Department of Anesthesiology, University of Munich, Medical Center Großhadern, Marchioninistrasse 15, W-8000 Munich, Federal Republic of Germany
[2]Department of Experimental Surgery, Surgical Clinic, University of Heidelberg, Im Neuenheimer Feld 347, W-6900 Heidelberg, Federal Republic of Germany

Received June 26, 1990 / accepted September 4, 1990

Summary. The quantitative analysis of the spatial variability of organ blood flow by means of radiolabeled microspheres (MS) requires that the methodological variability ("error") of the technique ($RD_{meth.}$) is known in each individual organ. Therefore, $RD_{meth.}$ was quantified (eight to nine nuclides) in 6941 tissue samples from 13 organs of three anesthetized dogs, and the relative importance of errors originating from both the stochastic nature of MS distribution ($RD_{theo.}$) and the process of quantitation of MS radioactivity ($RD_{counting}$) was assessed under varying conditions (high/low specific MS activity (SA_{MS}); inaccurate separation of gamma spectra; large sample size). At "minimized" methodological error (experiment 2), $RD_{meth.}$ of samples trapping ≈ 375 MS/nuclide was 5.8% and only slightly exceeded $RD_{theo.}$ (5%). $RD_{meth.}$ varied in the range 2.7–7.8% in individual organs and contributed little (3.5%) to the organs' observed spatial variability of flow. In contrast, $RD_{meth.}$ – due to increased $RD_{counting}$ – considerably exceeded $RD_{theo.}$ when SA_{MS} was low (experiment 3), overlap of two nuclides' main photopeaks was critical (experiment 1), or counting geometry was inappropriate (pulmonary tissue samples). At the same time, the contribution of $RD_{meth.}$ to spatial flow variability rose to 7.9% (experiment 3), 26.9% (experiment 1), and 15–23% (lungs). Completely artifactual measurements, as indicated by an extremely high $RD_{meth.}$ of sample flow, were rarely observed ($< 0.1\%$). In general, our data suggest that blood flow can be measured reproducibly and with low methodological error using up to 8 nuclides, $RD_{meth.}$ does not essentially contribute to the observed spatial variability of organ blood flow, and, hence, organ flow variability may be accurately quantified using the MS technique. However, if sources of error as indicated above are present, the practice of using $RD_{theo.}$ as a measure of $RD_{meth.}$ (thereby neglecting $RD_{counting}$)

* Part of this work was supported by the Deutsche Forschungsgemeinschaft, Sonderforschungsbereich 320, Project C3

Offprint requests to: B. Zwissler

may notably underestimate true MS error and result in an overestimation of spatial heterogeneity of organ blood flow. $RD_{meth.}$, therefore, should be quantified separately in each region of interest prior to the onset of a new study.

Key words: Radiolabeled microspheres – Methodological error – Organ blood flow – Blood flow distribution

Introduction

The microsphere (MS) technique is widely accepted for measuring cardiac output and its distribution to the organs of experimental animals [1, 19, 21]. More recently, the MS technique has also been used for the quantitative analysis of the spatial flow variability ($RD_{spat.}$) within the organs [10, 15, 22, 24, 25, 27, 28, 32]. This is achieved by dissecting the organ of interest into multiple samples, assessing the individual sample flows, and calculating $RD_{spat.}$ as the relative dispersion (RD) of these multiple sample-flow values ($RD_{spat.} = SD_{flow}/Mean_{flow}$). The knowledge of $RD_{spat.}$ obtained under varying experimental conditions is assumed to provide further insights into the regulatory mechanisms of capillary perfusion [10, 23–25, 27, 29].

It is known, however, that simultaneous flow measurements within a given tissue sample using multiple, differently radiolabeled MS of the same particle size do not yield identical values, but vary to a certain extent. This variability usually is addressed as the methodological error of the MS technique ($RD_{meth.}$). If $RD_{meth.}$ is high, this may pretend differences in sample flow where, in fact, no difference is present. Consequently, spatial flow variability may be observed ($RD_{spat.obs.}$), while true spatial variability ($RD_{spat.true}$) is actually absent [24]. Because $RD_{meth.}$ artificially contributes to $RD_{spat.obs.}$ according to the equation $RD^2_{spat.obs.} = RD^2_{spat.true} + RD^2_{meth.}$ [24], it follows that knowing $RD_{meth.}$ is crucial in all experiments designed to analyze $RD_{spat.true}$ using the MS technique.

In the past, the "theoretical" error ($RD_{theo.}$) mathematically derived from the MS content of a tissue sample [9], instead of the actually measured $RD_{meth.}$, has been indicated most often in the literature to delineate the methodological error of the MS technique [19, 21]. Yet, because $RD_{theo.}$ only encompasses variability of flow due to the stochastic nature of MS distribution (Poisson distribution) and does not include other major sources of error inherent to the process of quantitation of MS radioactivity (summarized as $RD_{counting}$), it may notably underestimate $RD_{meth.}$. Hence, $RD_{meth.}$ rather than $RD_{theo.}$ should be considered when the MS technique is used.

Up to now, however, $RD_{meth.}$ has been quantified only in the heart, lungs, and skeletal muscle [5, 15, 20, 22, 23, 27, 28, 32]; a comparison of $RD_{meth.}$ in the whole array of organs within the same experimental set-up has not yet been performed. This implies that in most of the organs $RD_{spat.true}$ has never been assessed. Moreover, the relative importance of both $RD_{counting}$ and $RD_{theo.}$ for explaining $RD_{meth.}$ in different organs and under varying conditions (high/low MS number in tissue samples, high/low specific MS activity, and inaccurate separation of gamma spectra) has not been investigated experimentally. Finally, no data are available with respect to the frequency of artifactual measurements inherent to the MS technique.

To study the above topics, blood flow was measured in a total of 6941 tissue samples from 13 organs of three anesthetized dogs. Up to nine differently radio-

labeled batches of MS were used simultaneously, and the mixture and specific activities of nuclides varied between the three experiments. This set-up made it possible to quantify $RD_{meth.}$ and assess the validity of $RD_{theo.}$ in predicting $RD_{meth.}$ in each individual tissue sample and organ, to quantify $RD_{counting}$ and its contribution to $RD_{meth.}$ under varying experimental conditions, to quantify $RD_{spat.obs.}$ and $RD_{spat.true}$ in 13 organs of the body, and to quantify the number of tissue samples presenting an extremely high $RD_{meth.}$, thereby estimating the frequency of artifacts occurring within the process of blood-flow measurements using radiolabeled MS.

By providing such data, we aimed to further characterize both the sources and the magnitude of the methodological errors inherent in the MS technique. This knowledge, in turn, is the prerequisite for accurately performing and correctly interpreting flow measurements obtained by means of the MS technique.

Materials and methods

Animal preparation

The study was performed with three foxhounds (male; 17, 18, 21 kg) premedicated with 0.75–1.00 mg/kg propiomazine (Combelen, Bayer, Leverkusen, FRG) and anesthetized with 20 mg/kg pentobarbital (Nembutal, Ceva, Bad Segeberg, FRG), 0.75 mg/kg piritramid (Dipidolor, Janssen, Neuss, FRG) and 0.25 mg/kg alcuronium (Alloferin, Roche, Grenzach-Wyhlen, FRG). Anesthesia was maintained by infusion of pentobarbital (5 mg/kg per h). The dogs were intubated and mechanically ventilated with 12 cycles/min using 100% O_2.

The descending aorta was cannulated via the left brachial artery to monitor arterial pressure. A Swan-Ganz catheter (7F, Edwards, Anasco, Puerto Rico) was inserted into the pulmonary artery to measure cardiac output (thermodilution) and pulmonary artery pressure as well as to withdraw the reference sample during pulmonary injection of MS. A tip manometer (PC 350, Millar Instruments, Houston, Tex., USA) was placed in the right ventricle. Under fluoroscopic control, a sidewinder catheter (6F, Cordis, Miami, Fla., USA) was passed via the right common carotid artery into the left atrium for systemic injection of MS. The right femoral artery was cannulated for the withdrawal of the arterial reference sample during the systemic MS injection. To obtain the blood needed for the 1:1 replacement of the amounts withdrawn for the reference samples, the animals were isovolemically hemodiluted with 6% dextran 60 (Macrodex; Schiwa, Glandorf, FRG) to a hematocrit of 28% and then allowed to stabilize for 30 min.

Microsphere methodology

To assess the methodological variability of the MS technique, MS labeled with different nuclides (^{141}Ce, ^{51}Cr, ^{103}Ru, ^{114m}In, ^{95}Nb, ^{47}Co, and ^{113}Sn with 16.5 ± 0.1 μm diameter; ^{46}Sc and ^{85}Sr with 16.5 ± 0.2 μm diameter; NEN-TRAC; DuPont, Wilmington, Del., USA) were injected simultaneously into the systemic (five or six nuclides) and pulmonary (three nuclides) circulation systems, respectively. MS number was adjusted to compensate for different decay rates and to achieve approximately equal fractions of nuclide activities; MS number averaged 430000 (range: 287000–750000) and 40000 (range: 33000–43000) MS/kg in the systemic and pulmonary injections, respectively.

In order to analyze the influence of a disturbed spectrum separation on the magnitude of the methodological error, we used two nuclides with similar main photopeaks (^{85}Sr at 514 keV and ^{103}Ru at 497 keV) in experiment 1, while spectrum separation error was minimized by omission of ^{85}Sr in experiments 2 and 3. To assess the impact of specific MS activity (SA_{MS}) on the methodological error, MS with different SA_{MS} were used in the three experiments (systemic injection): SA_{MS} averaged 11 (range: 5–20) counts per min per MS (cpm/MS) in experiment 1, 8 (range: 3–15) cpm/MS in experiment 2, but was only 3 (range: 1–5) cpm/MS in experiment 3.

For measurements, the MS were transferred into glass vials [21] and suspended in a saline solution having a total volume of ≈ 10 ml. The vials were vigorously agitated on a vortex mixer

Table 1. Dissection of organs and mean organ blood flow. Number of tissue samples obtained from each organ, mean sample weight, and mean organ blood flow on the basis of all experiments (mean ± SD). Because the number of tissue samples obtained from the heart, kidneys, and lungs – due to the dissection scheme applied in these organs – was slightly different in the three experiments, the range has been indicated

Organ flow	No. samples	Sample weight (g)	Organ blood (ml/min per g)
Gall bladder	6	0.34 ± 0.11	0.36 ± 0.07
Urinary bladder	10	1.40 ± 0.36	0.10 ± 0.04
Pancreas	20	2.09 ± 0.72	0.47 ± 0.06
Diaphragm	26	4.09 ± 1.10	0.10 ± 0.05
Skeletal muscle	36	4.12 ± 1.05	0.10 ± 0.04
Spleen	45	2.53 ± 1.05	0.61 ± 0.10
Bowel	125	4.32 ± 1.32	0.44 ± 0.04
Stomach	150	1.22 ± 0.77	0.43 ± 0.06
Brain	176	0.57 ± 0.33[a]	0.35 ± 0.04
Liver	265	2.34 ± 0.81	0.27 ± 0.08
Heart	494–502	0.24 ± 0.17[a]	0.90 ± 0.16
Kidneys	604–612	0.17 ± 0.07[a]	2.09 ± 1.04
Lungs	299–391	0.23 ± 0.19[b]	27.4 ± 10.9
Total	2264–2360		

[a] After fixation
[b] Dry weight

for at least 3 min. MS were then injected into the left atrium (systemic flow) within 20–30 s, while the vial was still being agitated manually. Similarly, for measurement of pulmonary flow, MS were injected in the right atrium 5 min later. No cardiorespiratory changes were observed following MS injection.

Reference samples were drawn from the abdominal aorta (systemic flow) and the pulmonary artery (pulmonary flow) over a 3-min period at a rate of 3.24 ml/min (Harvard Apparatus, South Natick, Mass., USA). The amounts of blood withdrawn were simultaneously and isovolemically replaced by autologous blood. Subsequent to MS injections, the animals were killed by i.v. injection of saturated potassium chloride solution and the organs removed. Prior to complete dissection, the heart, brain, and kidneys were fixed in 6% formaldehyde for 5–7 days, and the lungs were inflated and dried in room air for 4 days. The other organs were processed immediately. The number of tissue samples obtained from each organ and the mean sample weights are listed in Table 1.

The radioactivities of the tissue and reference samples were counted for 5 min each in a 1024-channel gamma counter (Model 5260; Packard Instruments, Downers Grove, Ill., USA) with a 3″ NaJ(Tl) detector and were analyzed as described elsewhere [16, 31]. Sample flow $\dot{Q}_{sample}$ (ml/min) (Heyman et al. [21]) was calculated for each nuclide as

$$\dot{Q}_{sample} = \dot{Q}_{ar} \cdot I_{sample}/I_{ar}, \quad (1)$$

where $\dot{Q}_{ar}$ = withdrawal rate of the arterial reference sample (ml/min). I_{ar} = counts/min in the arterial reference sample, and I_{sample} = counts/min in the tissue sample. $\dot{Q}_{sample}$ then was divided by the tissue weight and normalized to 1 g.

Methodological variability of blood-flow measurements

Methodological variability of the MS technique was quantified by calculating the relative dispersion of multiple, simultaneously measured sample-flow values as

$$RD_{meth.} = SD/Mean. \quad (2)$$

To summarize multiple values of $RD_{meth.}$, mean $RD_{meth.}$ was calculated as $(\Sigma RD^2_{meth.}/n)^{1/2}$, where n is the number of tissue samples.

According to Buckberg [9], a fraction of $RD_{meth.}$ is explained by the Poisson nature of MS distribution. This fraction was termed the theoretical methodological error ($RD_{theo.}$) of the MS technique, and was calculated as

$$RD_{theo.} = \sqrt{1/N}, \tag{3}$$

where N is the number of particles in the tissue sample regarding to a given nuclide. To calculate the mean $RD_{theo.}$ of a sample, an estimate of the average number of particles trapped in each individual tissue sample must be obtained. Because the number of MS used for simultaneous systemic injection varied considerably by a factor of 2.6 between the different nuclides, the weighted mean rather than the arithmetic mean of particles per sample was assessed as described by Bevington [7] and applied to the MS technique by Austin et al. [2].

Methodological variability not attributable to $RD_{theo.}$ originates from errors attributable to the quantitation of MS radioactivity (summarized as $RD_{counting}$). Assuming independence of errors, $RD_{counting}$ and $RD_{theo.}$ contribute to $RD_{meth.}$ as

$$RD^2_{meth.} = RD^2_{counting} + RD^2_{theo.}. \tag{4}$$

From Eq. 4, $RD_{counting}$ is derived as

$$RD_{counting} = \sqrt{RD^2_{meth.} - RD^2_{theo.}}. \tag{5}$$

Equation (4) defines to what extent both $RD^2_{couting}$ and $RD^2_{theo.}$ contribute to the total methodological variance of blood flow ($RD^2_{meth.}$). After normalizing $RD^2_{meth.}$ to a value of 100, these fractions are also available in terms of percent.

Spatial variability of blood flow

Each organ was dissected into a defined number of tissue samples yielding multiple (n) values of regional organ blood flow ($\dot{Q}_1, \dot{Q}_2, \ldots \dot{Q}_n$). Hence, the observed spatial variability of organ blood flow could be quantified by calculating the relative dispersion of $\dot{Q}_{1\ldots n}$ in each organ as

$$RD_{spat.obs.} = SD\ (\dot{Q}_{1\ldots n})/Mean\ (\dot{Q}_{1\ldots n}). \tag{6}$$

$RD_{spat.obs.}$ consists of the true spatial variability of organ blood flow ($RD_{spat.true}$) and $RD_{meth.}$ [24]. An additional error (ε) is introduced by the process of weighing and by differences in counting efficiency due to different sample geometry:

$$RD^2_{spat.obs.} = RD^2_{spat.true} + RD^2_{meth.} + \varepsilon. \tag{7}$$

For our equipment, weighing error was 0.1% (in samples of 200 mg) and counting efficiency (tested for ^{141}Ce, ^{51}Cr, ^{85}Sr, ^{95}Nb, and ^{46}Sc) was constant with 0.8–1.9% mean error in tissue samples ranging 0.5–4.5 cm in height within the counting vial (unpublished). Hence, ε was small compared with the values of $RD_{spat.obs.}$ and $RD_{meth.}$ measured in this study. Therefore, ε was neglected and $RD_{spat.obs.}$ was calculated as

$$RD^2_{spat.obs.} = RD^2_{spat.true} + RD^2_{meth.}. \tag{8}$$

Equation (8) defines to what extent both $RD^2_{spat.true}$ and $RD^2_{meth.}$ contribute to $RD^2_{spat.obs.}$. From Eq. (8), $RD_{spat.true}$ was calculated as

$$RD_{spat.true} = \sqrt{RD^2_{spat.obs.} - RD^2_{meth.}}. \tag{9}$$

Shunt flow

Systemic, pulmonary, and myocardial shunt flow was assessed by quantifying the number of particles appearing in mixed venous, arterial, and coronary sinus blood, respectively, and averaged 14.9 ± 0.6% (systemic shunt), 1.0 ± 0.6% (myocardial shunt), and 0.8 ± 0.5% (pulmonary shunt).

Results

Methodological error of the MS technique

Both the total methodological error of the MS technique ($RD_{meth.}$) and its contributing factors ($RD_{theo.}$, $RD_{counting}$) have been investigated under three different experimental conditions: critical overlap of two nuclides' main photo peaks in experiment 1; high specific MS activity in experiment 2; and low specific MS activity in experiment 3.

$RD_{meth.}$ and sample MS content. In Fig. 1, $RD_{meth.}$ of each individual tissue sample (dots) of experiments 1, 2, and 3 was plotted as a function of sample MS content and was compared with $RD_{theo.}$ (solid line). Figure 1 demonstrates, that $RD_{meth.}$ increased in all experiments as sample MS content decreased. In experiment 1, however, $RD_{meth.}$ showed large scatter and most of the values by far exceeded $RD_{theo.}$. In contrast, in experiments 2 and 3, $RD_{meth.}$ closely approximated $RD_{theo.}$ and scatter was low. $RD_{meth.}$ averaged 12.2%, 5.8%, and 7.9% (in experiments 1–3, respectively) in samples containing 350–400 MS ($RD_{theo.}$: $\approx 5\%$) and 11.4%, 3.1%, and 3.2% (in experiments 1–3, respectively) in samples with >2000 MS. Artificial measurements (characterized by an extremely high $RD_{meth.}$ and marked by an arrow in Fig. 1) occurred in seven samples, which were excluded from further analyses.

In Fig. 2, the relationship between $RD_{meth.}$ and sample MS content was separately analyzed in the heart, brain, and kidneys (data of experiments 2 and 3). Figure 2 demonstrates that there were no major differences between these organs either with respect to the slope of this function or in terms of absolute values of $RD_{meth.}$.

$RD_{counting}$ and sample MS content. In Fig. 3, the "counting" error ($RD_{counting}$) was depicted as a function of sample MS content. $RD_{counting}$ was much higher in experiment 1 than in experiments 2 and 3. $RD_{counting}$ was 11.1%, 2.9%, and 6.1% (in experiments 1–3, respectively) in samples containing 350–400 MS.

Methodological errors in different organs. Table 2 summarizes $RD_{meth.}$, $RD_{theo.}$ and $RD_{counting}$ as obtained in different organs. $RD_{meth.}$ was high in experiment 1 (7.9–14.5%), but was low in experiment 2 (2.7–7.8%) and slightly increased in experiment 3 (2.8–10.9%). $RD_{theo.}$ was 1.3–4.7% in experiment 1, 1.1–5.5% in experiment 2, and 1.4–7.1% in experiment 3. High $RD_{counting}$ was present in the organs of experiment 1 (7.6–13.7%), but was small in experiment 2 (0–5.9%) and moderate in experimenmt 3 (2.2–8.3%). In contrast, high $RD_{counting}$ and, hence, high $RD_{meth.}$ ($>13\%$) were encountered in pulmonary tissue of all three experiments.

From the data of Table 2, the relative contribution of $RD^2_{counting}$ to $RD^2_{meth.}$ may be calculated [Eq. (4)]. $RD^2_{counting}$ contributed to $RD^2_{meth.}$ between 78% (gallbladder) and 99% (pancreas) in experiment 1, between 0% (diaphragm) and 83% (spleen) in experiment 2, and between 40% (urinary bladder) and 85% (bowel) in experiment 3. Within the lungs, the contribution of $RD^2_{counting}$ to $RD^2_{meth.}$ averaged 97% in experiment 1, 92% in experiment 2, and 96% in experiment 3.

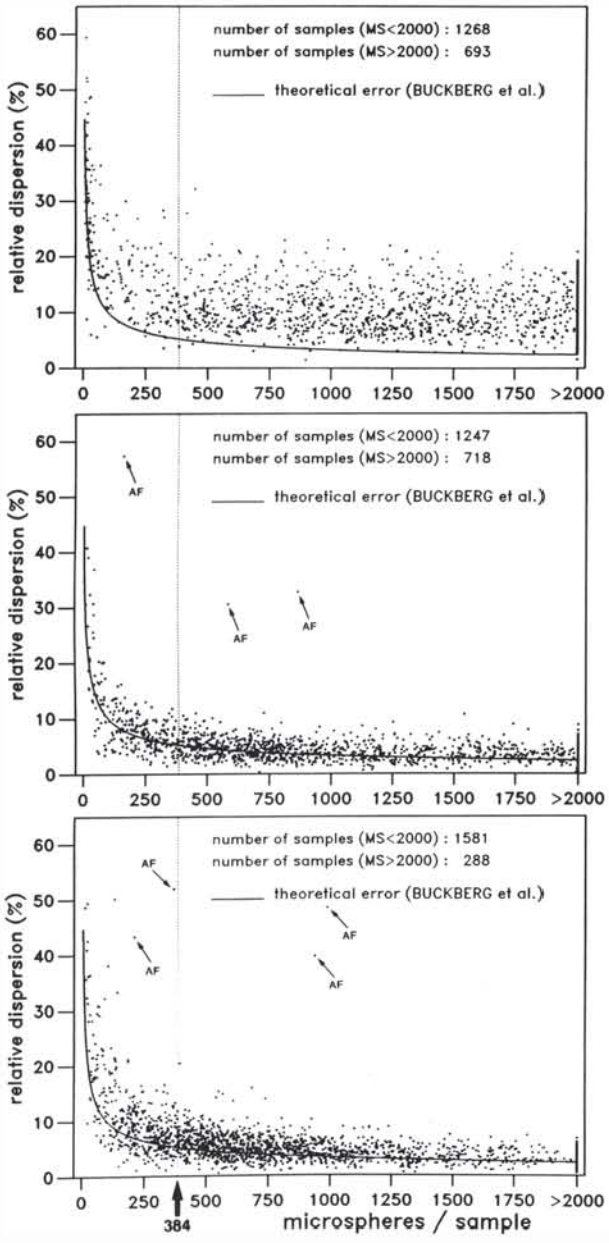

Fig. 1. Total methodological error of the MS technique as a function of sample MS content in different experiments. The total methodological error as observed in each individual sample of experiments 1–3 was plotted against the weighted mean number of MS/sample. Data from all samples (except the lungs) are shown. $RD_{meth.}$ of samples containing more than 2000 MS has been summed up at ">2000," where – due to the high number of samples – the dots run together into a straight line. Samples by far exceeding the normal scatter have been marked by *AF* (artifacts). $RD_{theo.}$ according to Buckberg et al. [9] has been included for means of comparison. $RD_{theo.}$ is 5% in samples trapping 384 MS *(dashed vertical line)*

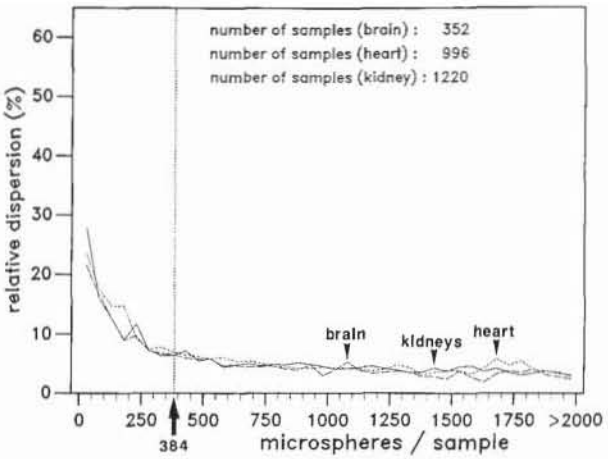

Fig. 2. Total methodological error of the MS technique as a function of sample MS content in different organs. The dependence of $RD_{meth.}$ on sample MS content was assessed separately in the *heart*, *brain*, and *kidneys*. For this purpose, samples of each experiment were classified according to their weighted mean MS content (0–50, 51–100, ... 1951–2000, >2000 MS/sample; 40 classes), mean $RD_{meth.}$ was calculated in each class and plotted against class. Data of experiments 2 and 3 were averaged. The slopes indicate that no difference exists between the organs with respect to $RD_{meth.}$ and its dependence on sample MS content

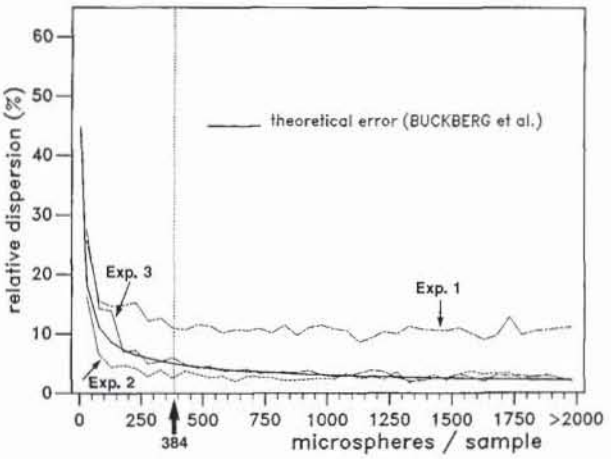

Fig. 3. "Counting" error as a function of sample MS content in different experiments. In each experiment, the error attributable to the process of quantitation of MS radioactivity was calculated and plotted as a function of the number of particles per sample. Data from all samples (except the lungs) are shown

Spatial variability of organ blood flow

As indicated in Table 2, $RD_{spat.obs.}$ ranged from 11.2% (spleen) to 63.9% (gallbladder) in experiment 1, from 7.2% (spleen) to 43.8% (gallbladder) in experiment 2, and from 8.7% (pancreas) to 68.3% (liver) in experiment 3. Only 3.5% (range: 0.5–14%, lungs excluded) of $RD^2_{spat.obs.}$ was attributable to $RD^2_{meth.}$ in experiment 2 [for calculation see Eq. (8)]. In contrast, $RD^2_{meth.}$ notably contributed to $RD^2_{spat.obs.}$ by 26.9% (range: 2.3–81.2%) in experiment 1 and within pul-

Table 2. Methodological and spatial variability of organ blood flow. For each organ and experiment, both the methodological error and the spatial variability of blood flow are indicated. $RD_{meth.}$ = total methodological error; $RD_{theo.}$ = theoretical methodological error; $RD_{counting}$ = error attributable to the process of quantification of MS radioactivity; $RD_{spat.obs.}$ = observed spatial variability of organ blood flow; $RD_{spat.true}$ = true spatial variability of organ blood flow

	Exp. no.	$RD_{meth.}$ (%)	$RD_{counting}$ (%)	$RD_{theo.}$ (%)	$RD_{spat.obs.}$ (%)	$RD_{spat.true}$ (%)
Bowel	1	8.5	8.4	1.3	36.7	35.7
	2	2.7	2.3	1.3	38.8	38.7
	3	3.6	3.3	1.4	21.2	20.9
Brain	1	14.5	13.7	4.7	40.3	37.6
	2	6.0	3.1	5.2	29.8	29.2
	3	7.9	5.7	5.5	40.4	39.6
Diaphragm	1	7.9	7.6	1.9	17.3	15.4
	2	3.1	0.0	3.1	29.0	28.8
	3	5.2	3.7	3.7	26.1	25.6
Gall bladder	1	9.6	8.5	4.5	63.9	63.2
	2	7.8	5.9	5.2	43.8	43.1
	3	10.9	8.3	7.1	38.6	37.1
Heart (left ventricle)	1	10.2	9.8	3.0	22.7	20.3
	2	5.3	3.1	4.3	27.7	27.2
	3	7.2	5.6	4.6	24.7	23.7
Kidneys (cortex)	1	12.0	11.6	3.2	31.4	29.1
	2	4.3	3.5	2.5	33.9	33.6
	3	6.9	4.9	4.9	24.7	23.7
Liver	1	12.4	12.3	1.8	19.8	15.5
	2	4.1	3.4	2.3	28.4	18.1
	3	6.1	5.1	3.4	68.3	68.1
Lung (right)	1	16.4	16.2	2.6	34.6	30.5
	2	13.9	13.3	3.8	36.3	33.5
	3	14.5	14.2	2.6	31.1	27.5
Lung (left)	1	20.2	19.9	3.5	40.5	35.1
	2	17.1	16.4	4.7	39.2	35.3
	3	15.0	14.6	3.3	34.4	31.0
Muscle	1	9.8	9.5	2.3	23.6	21.4
	2	3.9	1.6	3.6	28.5	28.2
	3	4.3	3.3	2.8	22.7	22.3
Pancreas	1	12.9	12.8	1.5	15.5	8.7
	2	3.1	2.1	2.2	14.5	14.1
	3	3.0	2.6	1.6	8.7	8.2
Spleen	1	10.1	10.0	1.4	11.2	4.8
	2	2.7	2.5	1.1	7.2	6.6
	3	2.8	2.2	1.7	9.6	9.2
Stomach (mucosa)	1	13.3	13.1	2.3	29.9	26.8
	2	3.1	1.6	2.6	22.9	22.7
	3	8.4	7.7	3.6	33.4	32.4
Urinary bladder	1	9.8	9.3	3.0	21.7	19.4
	2	6.1	2.7	5.5	34.9	34.4
	3	7.8	4.9	6.0	15.2	13.0

monary tissue (23%, 15%, and 20% in experiments 1, 2, and 3, respectively). In experiment 3, there was a moderate 7.8% (range: 0.8–26%) contribution of $RD^2_{meth.}$ to $RD^2_{spat.obs.}$. Despite $RD_{meth.}$ contributing to $RD_{spat.obs.}$, true spatial variability of blood flow was present in all organs and experiments and ranged from 4.8% (spleen) to 63.2% (gallbladder) in experiment 1, from 6.6% (spleen) to 43.1% (gallbladder) in experiment 2, and from 8.2% (pancreas) to 68.1% (liver) in experiment 3.

Discussion

Adequacy of the model

To minimize errors in flow measurements due to the experimental setup, the catheter for systemic MS injection was inserted into the left atrium rather than the left ventricle [21] and arterial reference blood was collected from the abdominal aorta rather than from the ascending aorta [3]. To prevent hypovolemia due to reference sample collection from affecting regional blood flow [33], during withdrawal, the blood was replaced simultaneously and isovolemically. Blood-flow values of the organs studied (Table 1) were similar to those reported by others in dogs [8, 12, 14, 15, 26, 29, 33].

Systemic shunt as observed in our experiments was higher than that reported in the literature for 15 μm MS [4, 17, 18] and may have resulted in erroneous values of nutritive blood flow and spatial flow variability. However, our data demonstrated negligible shunting in the heart and lungs. Similarly, no local shunting was found within the intestine despite the presence of notable systemic shunt (unpublished work from our laboratory). In accordance with the literature, we therefore believe that systemic shunting of MS – if present – occurs mainly within the skin, muscle, and fat tissue and, hence, should not have notably affected our data.

Factors contributing to the methodological error of the MS technique

Theoretical error. Recently, Dole et al. [11] reported that $RD_{meth.}$ increased as sample MS content decreased, and suggested that most of the error of the MS technique is explained by variability due to stochastic MS distribution ($RD_{theo.}$). Severe discrepancies between $RD_{meth.}$ and $RD_{theo.}$ in experiment 1 and – to a smaller degree – in experiment 3 of the present study indicate that this conclusion does not hold true when the specific MS activity is relatively low (experiment 3) or the accuracy and precision of gamma-spectrum separation is affected by critical photo-peak overlap (experiment 1).

Even in the absence of the above sources of variability, $RD_{meth.}$ exceeded $RD_{theo.}$ (experiment 2), suggesting the presence of errors other than the stochastic MS distribution. A low number of MS within the reference sample was shown to increase $RD_{meth.}$ [11]. However, this kind of error is negligible if more than 2000 MS are trapped [11], as was the case in our study. Therefore, it seems most likely that the difference between $RD_{meth.}$ and $RD_{theo.}$ was attributable to the error introduced by the process of quantifying MS radioactivity ($RD_{counting}$).

Counting error. In experiment 1, the simultaneous use of ^{85}Sr and ^{103}Ru resulted in a $RD_{meth.}$ of 12.2% in samples containing an average of 350–400 MS/nuclide.

thereby largely exceeding the $RD_{theo.}$ of 5% in this class. The discrepancy between $RD_{meth.}$ and $RD_{theo.}$ was due to a high $RD_{counting}$, which made up for 83% of the total methodological flow variability [Eq. (4)]. Hence, experiment 1 demonstrates that inappropriate separation of nuclides due to critical overlap of the photo peaks from only two out of nine nuclides elevated $RD_{meth.}$ to more than twice the value predicted by $RD_{theo.}$.

In experiments 2 and 3, ^{85}Sr had been omitted. In experiment 3, this resulted in a $RD_{meth.}$ of 7.9% in samples with 350–400 MS compared with the $RD_{theo.}$ of 5%. Similarly, Dole et al. [11] reported a $RD_{meth.}$ of 7.9% in samples with a $RD_{theo.}$ of 4.3% and – from the relatively small difference of 3.6% – concluded that errors in isotope quantitation do not notably contribute to $RD_{meth.}$. This conclusion does not consider, however, that $RD_{meth.}$ is not simply the sum of $RD_{theo.}$ and $RD_{counting}$, but the square root of the sum of $RD^2_{theo.}$ and $RD^2_{counting}$. According to this rule, $RD_{counting}$ calculated to 6.6% and accounted for $\approx 70\%$ of $RD^2_{meth.}$ in the experiments of Dole et al. Similarly, in experiment 3 of the present study, $RD_{counting}$ was 6.1% in samples with 350–400 MS, and thereby explained as much as 60% of $RD^2_{meth.}$ in this class.

While $RD_{counting}$ in experiment 3 was relatively high, it was low (2.9% at 350–400 MS/sample) and contributed little (25%) to $RD^2_{meth.}$ in experiment 2. This finding may be explained by the fact that radioactive decay is a Poisson random process, the variability of which contributes to $RD_{counting}$. Variability due to radioactive decay depends on the number of radioactive events ("counts") in a given tissue sample ($counts_{sample}$) and can be calculated as $RD_{decay} = \sqrt{1/counts_{sample}}$ [2]. Because $counts_{sample}$ is the product of specific MS activity, sample MS content, and counting time, RD_{decay} exponentially rises and, hence, increasingly contributes to $RD_{counting}$ as one or several of these variables decrease.

Since the experimental set-up of experiments 2 and 3 differed only with respect to specific MS activity, our data suggest that it was the divergent RD_{decay} that most probably explained why $RD_{counting}$, and consequently $RD_{meth.}$, deviated in both experiments.

Sample size. To examine whether sample size (weight) itself affects $RD_{meth.}$ independently of sample MS content, $RD_{meth.}$ was analyzed in samples of different weight (e.g., 0.1–0.3 g, 0.3–0.5 g, 0.5–0.7 g, 0.7–1.0 g), but similar MS content (e.g., 500 MS/sample). An identical $RD_{meth.}$ was found in all subgroups (e.g., 5.2%, 6.0%, 5.7%, and 6.1%, respectively, in experiment 2), indicating that sample weight per se does not affect $RD_{meth.}$. The fact that samples in the four classes differ substantially with respect to counting geometry, but not with respect to $RD_{meth.}$ supports the validity of the constant efficiency zone of our counting equipment.

In summary, flow measurements using up to eight different nuclides showed moderate $RD_{meth.}$ when the simultaneous use of ^{85}Sr and ^{103}Ru was avoided. $RD_{meth.}$ was independent from sample size. In contrast to previous work [11], we suggest that $RD_{counting}$ may make a notable ($\approx 25\%$ in samples with 350–400 MS) contribution to $RD_{meth.}$, even when the fractions of nuclides in the gamma spectrum are fairly balanced and specific MS activity is high. Because $RD_{theo.}$ underestimated $RD_{meth.}$ in all of our experiments, we conclude that $RD_{meth.}$ should be assessed in each laboratory prior to the onset of a new study. Furthermore, it should be noted that the drop in specific MS activity throughout an ex-

perimental series results in an exponential rise of RD_{decay} unless counting time is adequately adjusted. However, prolongation of counting time has practical limits if sample number is high. Another possibility for controlling RD_{decay} is to measure an identical number of radioactive events in each sample (fixed "count preset"). While the variable counting time implied with this technique may complicate the planning of the counting procedure, a fixed count preset guarantees an identical RD_{decay} throughout an experimental series. We, therefore, would prefer to reduce count preset and, hence, to accept a somewhat larger RD_{decay} for the benefit of knowing that the counting error is kept equal in all samples irrespective of the actual activity of specimens.

If the direct measurement of $RD_{meth.}$ is not possible, $RD_{meth.}$ must be estimated on theoretical grounds and an adequate experimental set-up (e.g., number of particles for injection, counting time, etc.) should be selected in order to confine $RD_{meth.}$ to an upper limit. Several algorithms are available for this purpose and are given in the Appendix. It should be noted, however, that an undue increase of $RD_{meth.}$ due to inappropriately high $RD_{counting}$ is not taken into account by this theoretical approach.

Methodological error in different organs

Although the MS technique is not limited to flow measurements in the heart, lungs, and skeletal muscle, reports on $RD_{meth.}$ are restricted to these organs [5, 15, 20, 22, 23, 27, 28, 32]. Therefore, the major aim of our study was to provide a survey of $RD_{meth.}$ as determined under identical experimental conditions in a wide range of organs. Considerable differences of the organs' $RD_{meth.}$ were found in our study. Because $RD_{meth.}$ tended to be relatively low in organs trapping many particles per sample, part of the differences of $RD_{meth.}$ were due to differences in the organs' $RD_{theo.}$. Our data provide evidence, however, that the mean organ-sample MS content is not the primary determinant of $RD_{meth.}$: even in several organs of experiment 2, $RD_{counting}$ exceeded $RD_{theo.}$, and hence made up for the major part of $RD_{meth.}$. The variation in magnitude of $RD_{counting}$ cannot be explained up to now, because flow measurements were performed simultaneously in all organs and the very same nuclides and technical equipment were used.

Large samples (up to 8 cm^3) were obtained from the inflated lungs. Counting of these specimens resulted in a $RD_{meth.}$ of 14–17% in experiment 2, which is higher than the $RD_{meth.}$ observed in the other organs of this experiment and the $RD_{meth.}$ found in homogenized pulmonary tissue [20]. Because our high $RD_{meth.}$ is not explained by randomness of MS distribution ($RD_{theo.} < 5\%$), inappropriate counting geometry due to large sample size most probably caused a rise of $RD_{meth.}$, which was similar in magnitude to that introduced by critical photopeak overlap, as seen in experiment 1.

Spatial variability of organ blood flow

While spatial variability ("heterogeneity") of organ blood flow is a well-known phenomenon, its etiology and physiological meaning are still the topics of many studies [10, 13, 15, 20, 24, 25, 27, 28, 30, 32]. In the present study, $RD_{spat.obs.}$ as measured in the heart, kidneys, and skeletal muscle was well within the range reported by others [10, 13, 15, 22–25, 27, 28, 30, 32]. $RD_{spat.obs.}$ for other organs

has been documented for the first time by this study and ranged from 7.2% (spleen, experiment 2) to 68.3% (liver, experiment 3)[1]. However, although the idea is tempting, $RD_{spat.obs.}$ of the various organs cannot be directly compared to each other. This is due to the more recent finding that the distribution of blood flow within the vascular network follows the rule that can be described by means of fractal geometry [6]. In more practical terms, this means that perfusion becomes more and more heterogeneous as observation moves from macrocirculation to microcirculation. Consequently, $RD_{spat.obs.}$ will increase as sample weight decreases [6]. This in turn means that $RD_{spat.obs.}$ cannot be directly compared except between organs dissected into samples of the same weight. For example, genuine spatial variability (on the level of the microcirculatory units) within the pancreas ($RD_{spat.obs.}$ of 14% in the present study) might in fact exceed that of the heart ($RD_{spat.obs.}$ of 23%), because average sample size was as high as 2.1 g in the pancreas, but as low as 0.24 g in the heart. The knowledge of the organs' fractal dimension D might be used to normalize $RD_{spat.obs.}$ to a standard sample weight of 1 g, resulting in direct comparability of these $RD_{spat.obs.}$ values [6].

In this context, a second methodological problem may occur in quantification of $RD_{spat.obs.}$. Owing to the exponential dependence of heterogeneity on sample weight, the presence of only a minor fraction of small tissue samples can lead to a major overestimation of $RD_{spat.obs.}$. Hence, it is advisable to dissect the organ into pieces as uniform as possible in order to obtain a narrow sample weight distribution.

A third drawback should be considered when interpreting $RD_{spat.obs.}$ data. If measured by the MS technique, $RD_{spat.obs.}$ may overestimate true spatial heterogeneity ($RD_{spat.true}$), because it always includes scatter due to $RD_{meth.}$, i.e., $RD^2_{spat.obs.} = RD^2_{spat.true} + RD^2_{meth.}$ [24]. Hence, the calculation of $RD_{spat.true}$ from $RD_{spat.obs.}$ requires that $RD_{meth.}$ is known. By measuring both $RD_{meth.}$ and $RD_{spat.obs.}$ simultaneously, we were able to assess the extent to which $RD_{meth.}$ contributed to $RD_{spat.obs.}$ in different organs. $RD_{spat.obs.}$ exceeded $RD_{meth.}$ in each organ of experiments 1–3, indicating that true spatial variability of flow was present. The small contribution of $RD^2_{meth.}$ to $RD^2_{spat.obs.}$ in experiments 2 and 3 (averaging 3.5% and 7.8%, respectively, in organs except lungs) suggests that, in general, $RD_{spat.obs.}$ does not notably overestimate $RD_{spat.true}$.

In drawing this conclusion, however, two aspects should be kept in mind. First, if $RD^2_{meth.}$ is increased due to inappropriately high "counting error," its contribution to $RD^2_{spat.obs.}$ may well reach 20–30%, thereby overestimating $RD^2_{spat.true}$ by the same amount. Second, because the level of spatial flow variability is negatively correlated to sample size independently of the methodological error (see above), the relative importance of $RD^2_{meth.}$ in contributing to $RD^2_{spat.obs.}$ may decrease as sample size decreases. Therefore, the high resolution of organ dissection and, hence, a high $RD^2_{spat.obs.}$ might explain the relatively small contribution of $RD^2_{meth.}$ to $RD^2_{spat.obs.}$ in the present study. In studies using rougher dissection schemes, the decrease of $RD_{meth.}$ (due to increased mean

[1] In the present study, $RD_{spat.obs.}$ has been quantified in three experiments, which might not be representative. However, in another series ($n = 8$) performed in our laboratory under identical experimental conditions (except that only one nuclide has been injected for blood-flow measurements), very similar values of $RD_{spat.obs.}$ have been obtained (mean ± SD): bowel 30.1 ± 4.4%, brain 35.8 ± 2.6%, diaphragm 33.7 ± 5.0%, gallbladder 36.9 ± 14.7%, heart (left ventricle) 24.2 ± 6.1%, kidneys (cortex) 38.1 ± 8.4%, liver 49.5 ± 13.4%, muscle 30.2 ± 8.7%, pancreas 14.6 ± 5.9%, spleen 12.8 ± 3.2%, stomach (mucosa) 36.9 ± 6.3%, and urinary bladder 34.7 ± 12.0%

sample MS content and reduced RD_{decay}) may be exceeded by the concomitant decrease of $RD_{spat.obs.}$. Consequently, the importance of $RD^2_{meth.}$ in explaining $RD^2_{spat.obs.}$ might rise, thereby possibly resulting in a notable overestimation of $RD^2_{spat.true}$. Because, in individual cases, both $RD^2_{meth.}$ and its contribution to $RD^2_{spat.obs.}$ cannot be anticipated, we suggest that these variables should be assessed before embarking on a detailed study of blood-flow distribution.

Artifactual measurements

Beyond the "normal" methodological variability, the MS technique may give rise to artifactual flow measurements due to clumping or incomplete mixing of MS [2, 21]. In the present study, artifactual measurements occurred at a rate of less than 0.1%, indicating that the MS technique is a highly reproducible method for measuring tissue blood flow.

In summary, there were four major findings of the present study:

1) Regional blood flow can be assessed with low frequency of artifactual measurements in the dog.
2) The methodological error of the MS technique is low if properly standardized and performed, and contributes little to the spatial variability of organ blood flow. In general, "heterogeneity" of blood flow therefore is not notably overestimated by the MS technique.
3) While true spatial flow variability was present in all organs examined, considerable inter-organ differences exist with respect to the magnitude of this phenomenon.
4) The practice of using $RD_{theo.}$ as a measure of $RD_{meth.}$ fails if high $RD_{counting}$ is present. Underestimation of $RD_{meth.}$ by $RD_{theo.}$ may result in false values and conclusions with respect to the true spatial heterogeneity of organ blood flow. In order to detect an unexpectedly high "counting" error, we suggest quantifying actual $RD_{meth.}$ separately in each region of interest prior to the onset of a new study.

References

1. Archie JP, Fixler DE, Ullyot DJ, Hoffman JIE, Utley JR, Carlson EL (1973) Measurement of cardiac output with and organ trapping of radioactive microspheres. J Appl Physiol 35:148–154
2. Austin RE Jr, Hauck WW, Aldea GS, Flynn AE, Coggins DL, Hoffman JIE (1989) Quantitating error in blood flow measurements with radioactive microspheres. Am J Physiol 257:H280–H288
3. Baer RW, Payne BD, Verrier ED, Vlahakes GJ, Molodowitch D, Uhlig PN, Hoffman JIE (1984) Increased number of myocardial blood flow measurements with radionuclide-labeled microspheres. Am J Physiol 246:H418–H434
4. Bartrum RJ, Berkowitz DM, Hollenberg NK (1974) A simple radioactive microsphere method for measuring regional blood flow and cardiac output. Invest Radiol 9:126–132
5. Bassingthwaighte JB, Malone MA, Moffett TC, King RB, Little SE, Link JM, Krohn KA (1987) Validity of microsphere depositions for regional myocardial flows. Am J Physiol 253:H184–H193
6. Bassingthwaighte JB, King RB, Roger SA (1989) Fractal nature of regional myocardial blood flow heterogeneity. Circ Res 65:578–590
7. Bevington PR (1969) Data reduction and error analysis for the physical sciences. McGraw-Hill, New York, pp 72–73, 113, 153–154
8. Beyer J, Meßmer K (1982) Organdurchblutung und Sauerstoffversorgung bei PEEP. (Anaesthesiol u Intensivmed 145) Springer, Berlin Heidelberg New York

9. Buckberg GD, Luck JC, Payne DB, Hoffman JIE, Archie JP, Fixler DE (1971) Some sources of error in measuring regional blood flow with radioactive microspheres. J Appl Physiol 31:588–604
10. Conway RS, Weiss HR (1985) Dependence of spatial heterogeneity of myocardial blood flow on mean blood flow rate in the rabbit heart. Cardiovasc Res 19:160–168
11. Dole WP, Jackson DL, Rosenblatt JI, Thompson WL (1982) Relative error and variability in blood flow measurements with radiolabeled microspheres. Am J Phyiol 243:H371–H378
12. Dorinsky PM, Hamlin RL, Gadek JE (1987) Alterations in regional blood flow during positive end-expiratory pressure ventilation. Crit Care Med 15:106–113
13. Falsetti HL, Carroll RJ, Marcus ML (1975) Temporal heterogeneity of myocardial blood flow in anesthetized dogs. Circulation 52:848–853
14. Fan FC, Schuessler GB, Chen RYZ, Chien S (1979) Determinations of blood flow and shunting of 9- and 15-μm spheres in regional beds. Am J Physiol 237:H25–H33
15. Franzen D, Conway RS, Zhang H, Sonnenblick EH, Eng C (1988) Spatial heterogeneity of local blood flow and metabolite content in dog hearts. Am J Physiol 254:H344–H353
16. Gross W, Schosser R, Messmer K (1990) MIC-III – An integrated software package to support experiments using the radioactive microsphere technique. Comput Methods Progr Biomed 33:65–85
17. Hales JRS (1973) Effects of exposure to hot environments on the regional distribution of blood flow and on cardiorespiratory function in sheep. Pflügers Arch 344:133–148
18. Hales JRS (1973) Radioactive microsphere measurement of cardiac output and regional tissue blood flow in the sheep. Pflügers Arch 344:119–132
19. Hales JRS (1989) Radioactive microsphere techniques for studies of the circulation. Clin Exp Pharmacol Physiol [Suppl 1]:31–46
20. Hedenstierna G, White FC, Wagner PD (1979) Spatial distribution of pulmonary blood flow in the dog with PEEP ventilation. J Appl Physiol 47:938–946
21. Heymann MA, Payne BD, Hoffman JE, Rudolph AM (1977) Blood flow measurements with radionuclide-labeled particles. Prog Cardiovasc Dis 20:55–79
22. Iversen PO, Nicolaysen G (1989) Heterogeneous blood flow distribution within single skeletal muscles in the rabbit: role of vasomotion, sympathetic nerve activity and effect of vasodilation. Acta Physiol Scand 137:125–133
23. Iversen PO, Standa M, Nicolaysen G (1989) Marked regional heterogeneity in blood flow within a single skeletal muscle at rest and during exercise hyperaemia in the rabbit. Acta Physiol Scand 136:17–28
24. King RB, Bassingthwaighte JB, Hales JRS, Rowell LB (1985) Stability of heterogeneity of myocardial blood flow in normal awake baboons. Circ Res 57:285–295
25. Kirkebø A, Haugan A, Tyssebotn I (1985) Blood flow heterogeneity in the renal cortex during burn shock in dogs. Acta Physiol Scand 123:205–213
26. Manny J, Justice R, Hechtman HB (1979) Abnormalities in organ blood flow and its distribution during positive end-expiratory pressure. Surgery 85:425–432
27. Marcus ML, Kerber RE, Ehrhardt J, Abboud FM (1975) Three dimensional geometry of acutely ischemic myocardium. Circulation 52:254–263
28. Marcus ML, Kerber RE, Ehrhardt JC, Falsetti HL, Davis DM, Abboud FM (1977) Spatial and temporal heterogeneity of left ventricular perfusion in awake dogs. Am Heart J 94:748–754
29. Piiper J, Pendergast DR, Marconi C, Meyer M, Heisler N, Cerretelli P (1985) Blood flow distribution in dog gastrocnemius muscle at rest and during stimulation. J Appl Physiol 58:2068–2074
30. Schanzenbächer P, Klocke FJ (1980) Inert gas measurements of myocardial perfusion in the presence of heterogeneous flow documented by microspheres. Circulation 61:590–595
31. Schosser R, Forst H, Gross W, Weiss C, Zeintl H, Messmer K (1987) Computer applications in surgical research. In: Baethmann A, Messmer K (eds) Surgical research: recent concepts and results. Springer, Berlin Heidelberg New York, pp 101–116
32. Sestier FJ, Mildenberger RR, Klassen GA (1978) Role of autoregulation in spatial and temporal perfusion heterogeneity of canine myocardium. Am J Physiol 235:H64–H71
33. Ritter C von, Hinder RA, Womack W, Bauerfeind P, Fimmel CJ, Kvietys PR, Granger DN, Blum AL (1988) Microsphere estimates of blood flow: methodological considerations. Am J Phyiol 254:G275–G279

Appendix

Assessment of optimal number of particles for injection

If tissue samples from multiple organs with largely differing flow rates and sample sizes are to be investigated, the assessment of the total MS dose ($MS_{tot.}$) needed for injection to preserve a certain, maximal methodological error (RD) may be difficult. In the following discussion, an algorithm is provided for calculating $MS_{tot.}$ (Fig. A1).

First, RD is defined by the investigator as a fraction of 1 (e.g., error = 5% → RD = 0.05) and the minimal number of particles ($MS_{min.}$) needed in a sample to preserve RD is determined using *one* of Eqs. (1)–(4) (Fig. A1). Equation (1) considers the Poisson nature of MS distribution as the only factor contributing to RD [9]. This assumption does not hold true under experimental conditions [2], but is often made and therefore has been included in the scheme as an option. Equation (2) considers the fact that both the radioactive decay and MS distribution are stochastic events, which add up to a combinded stochastic error [2]. Additional information on

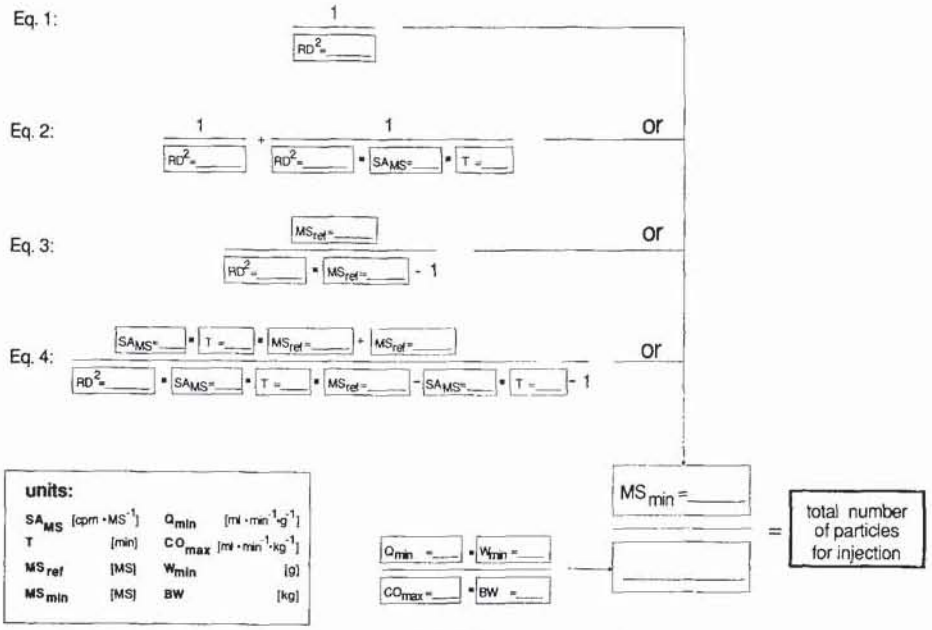

Fig. A1. Calculation of the total number of MS for injection. To calculate the total number of MS needed for injection, proceed as follows: (a) select the maximal methodological error you are willing to accept for your study. Division by 100 yields the *RD*, which is used for further calculations (e.g., error = 5% → RD = 0.05). (b) Insert the *RD* value into one of *Eqs. 1–4* (for selection see text) and calculate the minimal number of MS/sample ($MS_{min.}$) required to preserve the selected value of RD. In *Eqs. 2–4*, additional information must be added with respect to specific MS activity *(SA_{MS})*, counting time *(T)*, or the expected number of MS trapped in the reference sample *($MS_{ref.}$)*. (c) To obtain $MS_{tot.}$, divide $MS_{min.}$ by the term relating minimal expected sample flow *($Q_{min.}$)* and weight *($W_{min.}$)*, body weight *(BW)*, and maximal expected cardiac output *($CO_{max.}$)*. For example, let us assume the following values: maximal acceptable methodological error = 5% (i.e., $RD = 0.05$). $SA_{MS} = 2$ cpm/MS, $T = 2$ min, $MS_{ref.} = 1000$ particles, $BW = 20$ kg, maximal cardiac output = 100 ml/min per kg, $Q_{min.} = 1$ ml/min per g, and $W_{min.} = 0.3$ g. Under these conditions, the minimal number of MS needed to preserve RD calculates to 400 *(Eq. 1)*, 500 *(Eq. 2)*, 667 *(Eq. 3)*, and 1000 *(Eq. 4)*, respectively. Division of these data by the term as indicated yields a total MS dose for injection of 2.7, 3.3, 4.4, and $6.7 \cdot 10^6$ MS, respectively

specific MS activity (SA, counts/min per MS) and the selected counting time (t, min) are required to resolve Eq. (2), but are readily available in any laboratory. Equation (3) adds the arterial reference sample as a source of methodological variability. According to this equation, total methodological error is invoked by the Poisson nature of MS distribution in both the tissue and reference sample [11]. MS content within the reference sample ($MS_{ref.}$) depends on the total number of MS injected ($MS_{tot.}$), cardiac output (CO), and arterial reference withdrawal rate ($Q_{ar.}$), and can be assessed as $MS_{ref.} = MS_{tot.}/CO \cdot Q_{ar.}$. Because $MS_{tot.}$ is the end point of all calculations in the scheme, $MS_{ref.}$ has to be estimated at this step of the algorithm. In addition to Eq. (3), Eq. (4) (adapted according to Austin et al. [2]) includes the errors due to the Poisson distribution of radioactive decay in both the tissue and reference sample.

Equations (1)–(4) cannot anticipate errors due to nuclide separation and unequal counting efficiency. However, the present study as well as that of Austin et al. [2] have demonstrated that Eq. (4) only moderately underestimates the true methodological flow error. Eq. (4), therefore, is recommended for calculating $MS_{min.}$.

Beyond $MS_{min.}$, $MS_{tot.}$ depends on the animals' body weight (BW, kg), minimal expected sample weight ($W_{min.}$, g), minimal expected sample flow ($Q_{min.}$, $ml \cdot min^{-1} \cdot g^{-1}$), and maximal expected cardiac output ($CO_{max.}$, $ml \cdot min^{-1} \cdot kg^{-1}$), and can be derived as the flow ratio (R_{flow}) between $Q_{min.}$ and $CO_{max.}$, which is $R_{flow} = Q_{min.} \cdot 10^3/CO_{max.}$. The weight ratio ($R_{weight}$) between $W_{min.}$ and body weight is $R_{weight} = W_{min.} \cdot BW^{-1} \cdot 10^{-3}$, the factor of 10^3 in these equations being needed due to different units of weight (g, kg). Because the ratio between $MS_{min.}$ and $MS_{tot.}$ is proportional to R_{flow} and R_{weight} ($MS_{min.}/MS_{tot.} = R_{flow} \cdot R_{weight}$), $MS_{tot.}$ may be calculated (Fig. A1). In the algorithm shown in Fig. A1, BW and $MS_{min.}$ are known or may be calculated, while $W_{min.}$, $Q_{min.}$, and $CO_{max.}$ must be estimated or derived from the literature or own pilot studies.

In practice, $MS_{tot.}$ should be reduced if it exceeds the maximal single dose of MS (or, in the case of repetitive injections the maximal total MS dose divided by the number of injections) known to be tolerated without side effects by the species under investigation. In this case, sample size must be increased in order to preserve RD. Alternatively, the dissection scheme may be maintained if a higher RD is accepted for the study.